Trace metal imaging of sulfate-reducing bacteria and methanogenic archaea at single-cell resolution by synchrotron X-ray fluorescence imaging

Jennifer B. Glass[1*] *Si Chen*[2], *Katherine S. Dawson*[3], *Damian R. Horton*[1], *Stefan Vogt*[2], *Ellery D. Ingall*[1], *Benjamin S. Twining*[4], *Victoria J. Orphan*[3]

[1]School of Earth and Atmospheric Sciences, Georgia Institute of Technology, Atlanta, Georgia USA;

[2]Advanced Photon Source, Argonne National Laboratory, Argonne, Illinois, USA;

[3]Division of Geological and Planetary Sciences, California Institute of Technology, Pasadena, California, USA;

[4]Bigelow Laboratory for Ocean Sciences, East Boothbay, Maine, 04544, USA;

Keywords: sulfate reduction, methanogen, metals, methanol, synchrotron x-ray fluorescence

Running Head: Single-cell X-ray imaging

***Corresponding Author:** Jennifer.Glass@eas.gatech.edu

Abstract

Metal cofactors are required for many enzymes in anaerobic microbial respiration. This study examined iron, cobalt, nickel, copper, and zinc in cellular and abiotic phases at the single-cell scale for a sulfate-reducing bacterium (*Desulfococcus multivorans*) and a methanogenic archaeon (*Methanosarcina acetivorans*) using synchrotron x-ray fluorescence microscopy. Relative abundances of cellular metals were also measured by inductively coupled plasma mass spectrometry. For both species, zinc and iron were consistently the most abundant cellular metals. *M. acetivorans* contained higher nickel and cobalt content than *D. multivorans*, likely due to elevated metal requirements for methylotrophic methanogenesis. Cocultures contained spheroid zinc sulfides and cobalt/copper-sulfides.

Introduction

In anoxic natural and engineered environments, sulfate-reducing bacteria and methanogenic archaea perform the last two steps of organic carbon respiration, releasing sulfide and methane. Sulfate-reducing bacteria and methanogenic archaea can exhibit cooperative or competitive interactions depending on sulfate and electron donor availability (Brileya et al. 2014; Bryant et al. 1977; Ozuolmez et al. 2015; Stams and Plugge 2009). Methanol (CH_3OH), the simplest alcohol, is an important substrate for industrial applications (Bertau et al. 2014) and microbial metabolisms. In the presence of methanol, sulfate reduction and methanogenesis occur simultaneously in cocultures (Dawson et al. 2015; Phelps et al. 1985), anoxic sediments (Finke et al. 2007; Oremland and Polcin 1982), and anaerobic digesters (Spanjers et al. 2002; Weijma and Stams 2001). Methanol has also been studied as a substrate for stimulating organochlorine degradation in sediment reactors containing sulfate-reducing bacteria and methanogenic archaea (Drzyzga et al. 2002).

Metalloenzymes are essential for both sulfate reduction and methylotrophic methanogenesis (Barton et al. 2007; Ferry 2010; Glass and Orphan 2012; Thauer et al. 2010). Iron is needed for cytochromes and iron-sulfur proteins in both types of organisms (Fauque and Barton 2012; Pereira et al. 2011; Thauer et al. 2008). Cobalt and zinc are present in the first enzymes in sulfate reduction (ATP sulfurylase, Sat; Gavel et al. 1998; Gavel et al. 2008), and methylotrophic methanogenesis (methanol:coenzyme M methyltransferase; Hagemeier et al. 2006). Nickel is found in the final enzyme in methanogenesis (methyl coenzyme M reductase; Ermler et al. 1997), and zinc is present in the heterodisulfide reductase that recycles cofactors for the methyl coenzyme M reductase enzyme (Hamann et al. 2007). Nickel and cobalt are required by methanogenic archaea and sulfate-reducing bacteria that are capable of complete

organic carbon oxidization for carbon monoxide dehydrogenase/acetyl Co-A synthase in the Wood-Ljungdahl CO_2 fixation pathway (Berg 2011; Ragsdale and Kumar 1996). Hydrogenases containing Ni and Fe are functional in many, but not all, sulfate-reducing bacteria (Osburn et al. 2016; Pereira et al. 2011) and methylotrophic methanogens (Guss et al. 2009; Thauer et al. 2010). Evidence for high metabolic metal demands is provided by limited growth of methanogenic archaea without Co and Ni supplementation in methanol-fed monocultures (Scherer and Sahm 1981) and anaerobic bioreactors (Florencio et al. 1994; Gonzalez-Gil et al. 1999; Paulo et al. 2004; Zandvoort et al. 2003; Zandvoort et al. 2006).

Sulfate-reducing bacteria produce sulfide, which can remove toxic metals from contaminated ecosystems due to precipitation of metal sulfides with low solubility (Paulo et al. 2015). Metal sulfides may also limit the availability of essential trace metals for microbial metabolism (Glass and Orphan 2012; Glass et al. 2014). In sulfidic environments such as marine sediments and anaerobic digesters, dissolved Co and Ni are present in nanomolar concentrations (Glass et al. 2014; Jansen et al. 2005). These metals are predominantly present as solid metal sulfide precipitates (Drzyzga et al. 2002; Luther III and Rickard 2005; Moreau et al. 2013) and/or sorbed to anaerobic sludge (van Hullebusch et al. 2006; van Hullebusch et al. 2005; van Hullebusch et al. 2004). The bioavailability of metals in these solid phases to anaerobic microbes remains relatively unknown. Previous studies suggest that methanogenic archaea can leach Ni from silicate minerals (Hausrath et al. 2007) and metal sulfides (Gonzalez-Gil et al. 1999; Jansen et al. 2007). Sulfidic/methanogenic bioreactors (Jansen et al. 2005) and *D. multivorans* monocultures (Bridge et al. 1999) contain high-affinity Co-/Ni- and Cu-/Zn-binding ligands, respectively, which may aid in liberating metal micronutrients from solid phases when they become growth-limiting.

Due to the importance of trace metals for anaerobic microbial metabolisms in bioremediation and wastewater treatment, extensive efforts have focused on optimizing metal concentrations to promote microbial organic degradation in anaerobic digesters (for review, see Demirel and Scherer (2011)). Numerous studies have investigated the effect of heavy metals on anaerobic metabolisms at millimolar concentrations in heavy-metal contaminated industrial wastewaters, whereas few studies have investigated interactions between anaerobic microbes and transition metals at the low micro- to nanomolar metal concentrations present in most natural ecosystems and municipal wastewaters (see Paulo et al. 2015 for review). Studies of the metal content of anaerobic microbes have primarily measured monocultures using non-spatially resolved techniques such as ICP-MS (Barton et al. 2007; Cvetkovic et al. 2010; Scherer et al. 1983). Little is known about the effect of coculturing on cellular elemental composition and mineralogy due to changes in geochemistry (e.g. via sulfide production) of the medium and/or microbial metabolisms (e.g. via competition for growth-limiting substrates).

In this study, we measured cellular elemental contents and imaged extracellular metallic minerals for sulfate-reducing bacteria and methanogenic archaea grown in mono- and co-culture. For the model sulfate-reducing bacterium, we chose the metabolically versatile species *Desulfococcus multivorans*, which is capable of complete organic carbon oxidation. *Methanosarcina acetivorans* C2A, a well-studied strain capable of growing via aceticlastic and methylotrophic methanogenesis, but not on H_2/CO_2, was selected as the model methanogenic archaeon. These species were chosen because they are the most phylogenetically similar to pure culture isolates available to syntrophic consortia of anaerobic methanotrophic euryarchaeota (ANME-2) and sulfate-reducing bacteria (*Desulfosarcina/Desulfococcus*) partner that catalyze the anaerobic oxidation of methane in marine sediments (see Dawson et al. (2015) for more on

coculture design). Individual cells of mono- and cocultures of these two species were imaged for elemental content on the Bionanoprobe (Chen et al. 2013) at the Advanced Photon Source (Argonne National Laboratory) and measured for relative abundance of bulk cellular metals by ICP-MS.

Materials and Methods

Culture growth conditions

The growth medium contained (in g L^{-1}): NaCl, 23.4; $MgSO_4 \cdot 7H_2O$, 9.44; $NaHCO_3$, 5.0; KCl, 0.8; NH_4Cl, 1.0; Na_2HPO_4, 0.6; $CaCl_2 \cdot 2H_2O$, 0.14; cysteine-HCl, 0.25; resazurin, 0.001, 3 x 10^{-6} Na_2SeO_3 supplemented with DSM-141 vitamin (including 1 µg L^{-1} vitamin B_{12}) and trace element solutions containing metal concentrations (provided below as measured by ICP-MS) and 1.5 mg L^{-1} nitrilotriacetic acid (Atlas 2010). The medium (pH 7.6) was filter sterilized in an anoxic chamber (97% N_2 and 3% H_2 headspace) and reduced with 1 mM Na_2S.

Monocultures of *Desulfococcus multivorans* (DSM 2059) and *Methanosarcina acetivorans* strain C2A (DSM 2834) were inoculated into 20 mL culture tubes containing 10 mL of media with N_2:CO_2 (80:20) headspace, and sealed with butyl rubber stoppers and aluminum crimp seals. *D. multivorans* monocultures were amended with filter-sterilized lactate (20 mM). *M. acetivorans* monocultures were amended with filter-sterilized methanol (66 mM). Equal proportions of dense monocultures in early stationary stage (as assessed by OD_{600} measurements; Fig. S1) were inoculated into sterile media and amended with filter-sterilized lactate (20 mM) and methanol (66 mM) to form the coculture. Cultures were grown at 30°C without shaking. After 12 days of growth (Fig. S1), mono- and cocultures were pelleted and frozen for ICP-MS analysis, or prepared for SXRF imaging.

Fluorescence in situ hybridization

In order to confirm that monocultures were free of contamination, and to determine the relative abundance of *D. multivorans* and *M. acetivorans* in coculture, fluorescence *in situ* hybridization (FISH) was performed on separate aliquots from the same time point of the cell culture used for SXRF analyses. One mL of cell culture was preserved in 3% paraformaldehyde for 1-3 hours, then washed and resuspended in 200 µL of 3x PBS:ethanol as described in Dawson et al. (2012). Four microliters of fixed cells were spotted onto a glass slide and hybridized with an oligonucleotide probe targeting *Methanosarcina acetivorans* MSMX860 (Raskin et al. 1994) and the deltaproteobacterial probe Delta495a (Loy et al. 2002) and cDelta495a (Macalady et al. 2006). The FISH hybridization buffer contained 45% formamide, and the hybridization was carried out at 46°C for 2 hours followed by a 15 minute wash in 48°C washing buffer (Daims et al. 2005). The slides were rinsed briefly in distilled water, and mounted in a solution of DAPI (5 µg/mL) in Citifluor AF-1 (Electron Microscopy Services). Imaging was performed with a 100x oil immersion objective (Olympus PlanApo). Cell counts were performed by hand. Multiple fields of view from replicate wells were compiled and counted on the basis of fluorescence in DAPI (all cells), Cy3 (bacteria), and FITC (archaea).

ICP-MS

Frozen cell pellets were dried (yielding ~4 mg dry weight per sample) in acid-washed Savillex Teflon vials in a laminar flow hood connected to ductwork for exhausting acid fumes. Cells were digested overnight at 150°C in 2 mL of trace metal grade nitric acid and 200 µL hydrogen peroxide, dried again, and dissolved in 5 mL 5% nitric acid. The medium was diluted 1:50 in nitric acid. The elemental content of microbial cells and media was analyzed by ICP-MS (Element-2, University of Maine Climate Change Institute). Sterile medium contained the

following concentrations (in μM): P, 800; Zn, 7; Fe, 4; Co, 2; Ni, 0.9; Cu, 0.3. Digestion acid blanks contained (in nM): P, 127; Zn, 12; Fe, 5; Co, 0.007; Ni, 0.9; Mo, 0.02; Cu, 0.1; V, 0.03.

SXRF sample preparation

Monocultures were prepared for SXRF analysis without chemical fixation by spotting onto silicon nitride (SiN) wafers (Silson Ltd., cat. 11107126) followed by rinsing with 10 mM HEPES buffer (pH 7.8). To enable FISH microscopy after SXRF analysis, cocultures were chemically preserved prior to analysis by incubation on ice for 1 hour in 50 mM HEPES and 0.6 M NaCl (pH 7.2) containing 3.8% paraformaldehyde and 0.1% glutaraldehyde that had been cleaned of potential trace-metal contaminants with cation exchange resin (Dowex 50-W X8) using established protocols (Price et al. 1988; Twining et al. 2003). Cells were then centrifuged, re-suspended in 10 mM HEPES buffer (pH 7.8) and either embedded in resin and thin sectioned following the methods described in McGlynn et al. (2015) or spotted directly onto SiN wafers.

SXRF analyses

Whereas ICP-MS measurements cannot delineate the elemental contributions of co-occurring cell types, SXRF imaging enables elemental quantification of the specific cell of interest (Fahrni 2007; Ingall et al. 2013; Kemner et al. 2004; Nuester et al. 2012; Twining et al. 2003; Twining et al. 2008). SXRF analyses were performed at the Bionanoprobe (beamline 21-ID-D, Advanced Photon Source, Argonne National Laboratory). Silicon nitride wafers were mounted perpendicular to the beam as described in Chen et al. (2013). SXRF mapping was performed with monochromatic 10 keV hard X-rays focused to a spot size of ~100 nm using Fresnel zone plates. Concentrations and distributions of all elements from P to Zn were analyzed in fine scans using a step size of 100 nm and a dwell time of 150 ms. An X-ray fluorescence thin film (AXO DRESDEN, RF8-200-S2453) was measured with the same beamline setup as a reference. MAPS

software was used for per-pixel spectrum fitting and elemental content quantification (Vogt 2003). Sample elemental contents were computed by comparing fluorescence measurements with a calibration curve derived from measurements of a reference thin film.

Regions of interest (ROIs) were selected with MAPS software by highlighting each microbial cell (identified based on elevated P content with care taken to avoid regions of elevated non-cellular metals) or particle (identified based on elevated metal content). Each ROI (n=14 and n=17 for *D. multivorans* (radius: 0.60 ± 0.01 μm) and *M. acetivorans* (radius: 0.48 ± 0.01 μm), respectively, and n=13 for the coculture (radius: 0.96 ± 0.01 μm)) was background corrected to remove elements originating from each section of the SiN grid on which cells were spotted. To do so, the mean of triplicate measurements of area-normalized elemental content for blank areas bordering the analyzed cells was subtracted from cellular ROIs. The background-corrected area-normalized molar elemental content was then multiplied by cellular ROI area to obtain molar elemental content per cell, which was then divided by the cell volume ($4/3\pi r^3$, assuming spherical cells) to yield total metal content per cell volume, in units of mmol L^{-1}. Visualization of elemental co-localization was performed with MAPS software. Statistical analysis was performed with JMP Pro (v. 12.1.0) using the Tukey-Kramer HSD test.

Results

Cellular elemental content of monocultures

Cellular metal contents of *M. acetivorans* and *D. multivorans* monocultures followed the trend Zn ≈ Fe > Cu > Co > Ni when measured by SXRF, and Zn ≈ Fe > Co > Ni > Cu when measured by ICP-MS (Fig. 1). When normalized to cell volume, cellular S measured by SXRF was 50x higher in methanol-grown *M. acetivorans* (n=14) than lactate-grown *D. multivorans* (n=17).

185 Cellular P, Fe, Co, Ni and Cu were 4-7x higher in *M. acetivorans* than *D. multivorans*, and
186 cellular Zn was not significantly different between the two microbes (Table 1).

187 ***Relative abundance of species in coculture***

188 Coculturing of both species for 12 days in media containing methanol and lactate resulted in
189 dominance of *M. acetivorans* (77%, or 1,753 cells hybridized with the MSMX860 FISH probe)
190 over *D. multivorans* (23%, or 522 cells hybridized with the Delta495a FISH probe) for 2,275
191 total cells counted in ten 100x (125 x 125 μm) fields of view. Cells were ~1 μm^2 cocci. No other
192 cells exhibited DAPI staining other than those that hybridized with MSMX860 and Delta495a
193 oligonucleotide probes. Attempts at FISH microscopy after SXRF analysis were unsuccessful
194 due to x-ray radiation damage of the cells.

195 ***Cellular elemental content of cocultures***

196 ICP-MS measurements showed that the relative abundance of cellular metals remained relatively
197 constant between mono- and cocultures, whereas SXRF data indicated that the coculture
198 contained a relatively higher proportion of Co than the monocultures (Fig. 1). SXRF imaging
199 showed no visual difference in elemental distribution between cells in the coculture (Fig. 2),
200 although the relatively small size of the cells relative to the focused x-ray spot may have limited
201 our ability to discern subtle differences. Cocultures, which were fixed with paraformaldehyde
202 and glutaraldehyde for subsequent fluorescence microscopy, were larger (radius: 0.96 ± 0.01
203 μm) than monocultures (*D. multivorans* radius: 0.60 ± 0.01 μm; *M. acetivorans* radius: 0.48 ±
204 0.01 μm), which were not fixed prior to analysis. When normalized on a per cell basis,
205 cocultures contained 5-20x higher P, Co and Ni than monocultures; however, when normalized
206 to cellular volume, the larger cell volumes of the cocultures resulted in significantly less Fe, Cu
207 and Zn per cellular volume than either of the monocultures (Table 1).

208 ***Non-cellular metals in cocultures***

209 In whole cell SXRF images, ~30 "hot spots" (discrete semi-circular areas with low-P and
210 elevated metals, indicative of nano-sized minerals) of Zn (max: 0.7 μg cm^{-2}), Co (max: 0.4 μg
211 cm^{-2}) and S (max: 2.7 μg cm^{-2}) were present in the center of a cluster of ~30 cocultured cells
212 identified as P-containing cocci (Fig. 2). In thin sections, semi-circular non-cellular small Zn hot
213 spots (0.6 ± 0.1 μm^2) containing ~1:1 molar ratios of Zn:S (17 ± 2 μg Zn cm^{-2}: 7.6 ± 0.7 μg S
214 cm^{-2}) were interspersed amongst cell clusters (n=8; Fig. 3a-e) along with more numerous
215 spheroid non-cellular Co hot spots of the same size (0.6 ± 0.1 μm^2) containing 2.1 ± 0.1 μg Co
216 cm^{-2}, 3.4 ± 0.2 μg S cm^{-2}, and 1.3 ± 0.1 μg Cu cm^{-2} (n=45; Fig. 3a-e). Discrete semi-circular hot
217 spots of elevated Ni (max: 2.9 μg cm^{-2}) with low S were observed in two imaging fields (n=8;
218 Fig. 3b,c).

219

220 **Discussion**

221 In this study, SXRF imaging and quantification of trace metals in cellular and abiotic phases was
222 performed at the single-cell scale. Our observation that Zn and Fe were the two most abundant
223 cellular trace metals in monocultures is consistent with previous studies of diverse prokaryotes
224 (Barton et al. 2007; Cvetkovic et al. 2010; Outten and O'Halloran 2001; Rouf 1964), including
225 diverse mesophilic and hyperthermophilic methanogens grown on a range of substrates, for
226 which, generally: Fe > Zn > Ni > Co > Cu (Cameron et al. 2012; Scherer et al. 1983). To our
227 knowledge, there are no previous reports of the trace metal content of sulfate-reducing bacteria,
228 but the abundance of Fe and Zn-containing proteins encoded by their genomes (Barton and
229 Fauque 2009; Barton et al. 2007; Fauque and Barton 2012) is consistent with the cellular
230 enrichment we observed in these trace metals.

231 Both normalizations for SXRF data (per cell and per cellular volume) showed that the
232 methanogenic archaeon contained more P, S, Co, Ni and Cu than the sulfate-reducing bacterium.
233 The higher cellular Co content of *M. acetivorans* vs. *D. multivorans* is likely due to due to
234 numerous methyltransferases involved in methylotrophic methanogenesis (Zhang and Gladyshev
235 2010; Zhang et al. 2009) that contain cobalt as a metal center in their corrinoid (vitamin B_{12})
236 cofactor, in addition to the corrinoid-containing Fe-S methyltransferase protein in the Wood
237 Ljungdahl pathway in both species (Ekstrom and Morel 2008; Fig. 4). Similarly, the higher Ni
238 content of *M. acetivorans* vs. *D. multivorans* is likely due to the presence of Ni-containing
239 cofactor F_{430} in methyl coenzyme M reductase, the final enzyme in the methanogenesis pathway.
240 Cofactor F_{430} is found only in methane-metabolizing archaea, in which it comprises 50-80% of
241 total cellular Ni (Diekert et al. 1981; Mayr et al. 2008). Additional Ni requirements in both *M.*
242 *acetivorans* and *D. multivorans* are used for Ni-Fe hydrogenases and carbon monoxide
243 dehydrogenase in the Wood-Ljungdahl pathway (Fig. 4).
244 Metabolic Cu requirements for methanogenesis are not well known, although high
245 accumulations have also been reported for other methanogens (Scherer et al. 1983). However, it
246 should be noted that our early trials analyzing S-rich cells on Au grids revealed artifacts resulting
247 from interactions of S and Cu underlying the grid's surface Au coating (data not shown); use of
248 SiN grids in this study appeared to eliminate such Cu artifacts, but potential reactions between
249 trace Cu in SiN grids and abundant S in the archaeal cells cannot be completely discounted.
250 Faster growth rates of methylotrophic methanogens than sulfate-reducing bacteria at
251 moderate temperatures have been reported in previous studies (Dawson et al. 2015; Weijma and
252 Stams 2001), and likely account for *M. acetivorans* outcompeting *D. multivorans* in our
253 cocultures. We consider it unlikely that differences in cellular trace metal contents in

monocultures were a result of harvesting *D. multivorans* earlier in their stationary phase than *M. acetivorans* (Fig. S1) because cellular metal reserves generally decline or remain constant in stationary phase (Bellenger et al. 2011). Our SXRF measurements of cocultures are more difficult to interpret due to apparent swelling of aldehyde-fixed cocultured cells (~1 μm radius) to ~2x the size of monocultures (0.5-0.6 μm radius). When normalized per cell, fixed cocultures showed significantly higher P, Co and Ni than unfixed monocultures, but the apparent swelling of cocultured cells erased this trend when normalized to cellular volume.

When grown at millimolar metal concentrations, sulfate-reducing bacteria efficiently remove metals from solution (Krumholz et al. 2003) and precipitate covellite (CuS; Gramp et al. 2006; Karnachuk et al. 2008), sphalerite/wurtzite (ZnS/(Zn,Fe)S; Gramp et al. 2007; Xu et al. 2016), and pentlandite (Co_9S_8) (Sitte et al. 2013). Based on its ~1:1 Zn:S ratio, the semi-circular nanoparticulate zinc sulfide phase(s) observed in thin sections imaged by SXRF in this study were likely sphalerite spheroids, also found in sulfate-reducing bacteria biofilms due to aggregation of ZnS nanocrystals (0.1-10 μm) and extracellular proteins (Moreau et al. 2004; Moreau et al. 2007). The abiotic phase with the approximate stoichiometry $(CoCu)S_2$ may be mineralogically distinct from those in previous studies.

Conclusions and Challenges

This study used two independent methods for assessing trace metal inventories in anaerobic microbial cultures. We found that SXRF is a promising method for imaging and quantifying first-row transition metals in anaerobic microbial cultures at single-cell resolution. This method's single-cell resolution enables more precise measurements of cellular metal content than ICP-MS analysis of bulk cells, which can include metals bound to extracellular aggregations such as

277 cation-binding exopolymeric substances produced by sulfate-reducing bacteria (Beech and
278 Cheung 1995; Beech et al. 1999; Braissant et al. 2007). We did not observe evidence of metal
279 contamination from aldehyde fixation in SXRF data, likely because we pre-cleaned fixatives
280 with metal-chelating resin prior to use, as previously described by Twining et al. (2003).

281 Challenges remain with accurate elemental quantification of microbial cocultures
282 preserved in a manner that would also allow assignment of identity for similar cell types. It was
283 not possible to distinguish methanogenic archaea from sulfate-reducing bacteria in coculture on
284 the basis of cell morphology or elemental content, and attempts to image cells with fluorescent
285 oligonucleotide probes after SXRF analysis were unsuccessful due to x-ray radiation damage.
286 We recommend method development for simultaneous taxonomic identification and elemental
287 imaging (e.g. gold-FISH (Schmidt et al. 2012)) for samples containing multiple microbial
288 species as a high priority for future work.

Author Contributions

J.B.G., V.J.O., S.C., and K.S.D. conceived and designed the experiments; K.S.D. performed the microbial culturing, S.C., J.B.G., and S.V. performed the SXRF analyses; B.S.T. performed the ICP-MS analysis, J.B.G., S.C., D.R.H., S.V., E.D.I., and B.S.T. analyzed the data; and J.B.G. wrote the manuscript with input from all authors. All authors have given approval to the final version of the manuscript.

Funding Sources

This work was supported by a NASA Astrobiology Postdoctoral Fellowship to J.B.G, NASA Exobiology award NNX14AJ87G to J.B.G., DOE Biological and Environmental Research award DE-SC0004949 to V.J.O, and NSF award OCE-0939564 to V.J.O. Use of the Advanced Photon Source, an Office of Science User Facility operated for the U.S. DOE Office of Science by Argonne National Laboratory, was supported by the U.S. DOE under Contract No. DE-AC02-06CH11357. Use of the LS-CAT Sector 21 was supported by the Michigan Economic Development Corporation and the Michigan Technology Tri-Corridor (Grant 085P1000817). We thank two anonymous reviewers for helpful feedback on the previous version of this manuscript.

Acknowledgements

We thank Shawn McGlynn for assistance with sample preparation, and Keith Brister, Junjing Deng, Barry Lai and Rachel Mak at LS-CAT for assistance with Bionanoprobe analysis. We thank Larry Barton and Joel Kostka for helpful discussions, and Marcus Bray, Amanda Cavazos, Grayson Chadwick, Chloe Stanton, and Nadia Szeinbaum for feedback on previous manuscript drafts.

311 **Table 1.** Mean and standard error (in parentheses) of elemental contents normalized per cellular
312 volume and per cell as measured by SXRF. Monocultures were prepared without chemical
313 fixation, and cocultures were prepared with paraformaldehyde and glutaraldehyde fixation,
314 followed by spotting onto silicon nitride wafers as described in the text. A, B and C superscripts
315 indicate statistically different elemental contents ($p < 0.05$ based on Tukey-Kramer HSD test).

Culture	Substrate (mM)	P	S	Fe	Co	Ni	Cu	Zn
		Element per cellular volume (mmol L^{-1})						
100% *Methanosarcina acetivorans* DSM 2834 (n = 14)	Methanol (66 mM)	382^{A} (47)	4553^{A} (458)	38^{A} (4)	3.1^{A} (0.3)	0.44^{A} (0.04)	11^{A} (1)	38^{A} (3)
100% *Desulfococcus multivorans* DSM 2059 (n = 17)	Lactate (20 mM)	55^{B} (7)	96^{B} (11)	22^{B} (4)	0.5^{B} (0.1)	0.11^{B} (0.02)	3^{B} (1)	36^{A} (10)
77% *Methanosarcina acetivorans* DSM 2834, 23% *Desulfococcus multivorans* DSM 2059 (n = 13)	Methanol (66 mM), lactate (20 mM)	353^{A} (32)	234^{B} (19)	3.6^{C} (0.3)	2.0^{C} (0.2)	0.15^{B} (0.01)	0.13^{C} (0.04)	2.4^{B} (0.2)
		Element per cell (mol x 10^{-18} $cell^{-1}$)						
100% *Methanosarcina acetivorans* DSM 2834 (n = 14)	Methanol (66 mM)	178^{A} (28)	2167^{A} (318)	19^{A} (4)	1.5^{A} (0.2)	0.20^{A} (0.03)	5^{A} (1)	17^{AB} (2)
100% *Desulfococcus multivorans* DSM 2059 (n = 17)	Lactate (20 mM)	60^{A} (11)	107^{B} (19)	24^{A} (6)	0.5^{A} (0.1)	0.12^{A} (0.02)	3^{A} (1)	39^{A} (12)
77% *Methanosarcina acetivorans* DSM 2834, 23% *Desulfococcus multivorans* DSM 2059 (n = 13)	Methanol (66 mM), lactate (20 mM)	1252^{B} (69)	855^{C} (69)	13^{A} (1)	7^{B} (1)	2^{B} (1)	0.5^{B} (0.2)	9^{B} (1)

316

Figure Captions

Figure 1. Proportions of each cellular metal (Fe, Co, Ni, Cu and Zn) for monocultures of *Methanosarcina acetivorans* (n=14), monocultures of *Desulfococcus multivorans* (n=18), and cocultures of 77% *M. acetivorans* and 23% *D. multivorans* (n=12) measured by ICP-MS (bulk measurement) and SXRF (single cell average).

Figure 2. SXRF co-localization of P (red), Co (green), and Zn (blue; left panel), and S (red), Ni (green), and Cu (blue; right panel) for whole cells of 77% *Methanosarcina acetivorans* and 23% *Desulfococcus multivorans* in coculture. Values in parentheses are maxima in μg cm^{-2} for each element.

Figure 3. SXRF co-localization of P (red), Co (green), and Zn (blue) in left panels, and S (red), Ni (green), and Cu (blue) in right panels for five imaged fields of 5 μm thin sections of 77% *Methanosarcina acetivorans* and 23% *Desulfococcus multivorans* cocultures. Values in parentheses are maxima in μg cm^{-2} for each element.

Figure 4. Schematic of metalloenzyme-containing metabolic pathways in the complete carbon-oxidizing sulfate-reducing bacterium *Desulfococcus mutitvorans* and the methylotrophic methanogenic archaeon *Methanosarcina acetivorans* as confirmed by genomic analyses. Nickel (Acs, Cdh, Mcr) and cobalt (CFeSP, Mts, Mtr, and Sat) containing enzymes are labeled in bold. Enzyme abbreviations: Acs/CFeSP: acetyl-CoA synthase/corrinoid-FeS protein; Cdh: carbon monoxide dehydrogenase; Mts: methanol:coenzyme M methyltransferase; Mcr: methyl coenzyme M reductase; Mtr: methyl-tetrahydromethanopterin:coenzyme M methyltransferase; Sat: ATP sulfurylase.

338 **Figure S1.** Growth curves based on OD600 for the three cultures described in this study:
339 *Methanosarcina acetivorans* (white), *Desulfococcus multivorans* (light grey), and 77%
340 *Methanosarcina acetivorans* and 23% *Desulfococcus multivorans* cocultures (dark grey).
341

References

Atlas RM. 2010. Handbook of Microbiological Media. CRC press.

Barton LL, Fauque GD. 2009. Biochemistry, physiology and biotechnology of sulfate□reducing bacteria. Adv Appl Microbiol 68:41-98.

Barton LL, Goulhen F, Bruschi M, Woodards NA, Plunkett RM, Rietmeijer FJM. 2007. The bacterial metallome: composition and stability with specific reference to the anaerobic bacterium *Desulfovibrio desulfuricans*. Biometals 20:291–302.

Beech I, Cheung CS. 1995. Interactions of exopolymers produced by sulphate-reducing bacteria with metal ions. Int Biodeter Biodegr 35(1):59-72.

Beech I, Zinkevich V, Tapper R, Gubner R, Avci R. 1999. Study of the interaction of sulphate-reducing bacteria exopolymers with iron using X-ray photoelectron spectroscopy and time-of-flight secondary ionisation mass spectrometry. J Microbiol Met 36(1):3-10.

Bellenger JP, Wichard T, Xu Y, Kraepiel AML. 2011. Essential metals for nitrogen fixation in a free living N2 fixing bacterium: chelation, homeostasis and high use efficiency. Environ Microbiol 13(6):1395–1411.

Berg IA. 2011. Ecological aspects of the distribution of different autotrophic CO2 fixation pathways. Appl Environ Microbiol 77(6):1925-1936.

Bertau M, Offermanns H, Plass L, Schmidt F, Wernicke H-J. 2014. Methanol: the basic chemical and energy feedstock of the future. Springer.

Braissant O, Decho AW, Dupraz C, Glunk C, Przekop KM, Visscher PT. 2007. Exopolymeric substances of sulfate□reducing bacteria: interactions with calcium at alkaline pH and implication for formation of carbonate minerals. Geobiology 5(4):401-411.

Bridge TA, White C, Gadd GM. 1999. Extracellular metal-binding activity of the sulphate-reducing bacterium *Desulfococcus multivorans*. Microbiology 145(10):2987-2995.

Brileya KA, Camilleri LB, Zane GM, Wall JD, Fields MW. 2014. Biofilm growth mode promotes maximum carrying capacity and community stability during product inhibition syntrophy. Front Microbiol 5:693.

Bryant M, Campbell LL, Reddy C, Crabill M. 1977. Growth of *Desulfovibrio* in lactate or ethanol media low in sulfate in association with H2-utilizing methanogenic bacteria. Appl Environ Microbiol 33(5):1162-1169.

Cameron V, House CH, Brantley SL. 2012. A first analysis of metallome biosignatures of hyperthermophilic archaea. Archaea 2012:12.

Chen S, Deng J, Yuan Y, Flachenecker C, Mak R, Hornberger B, Jin Q, Shu D, Lai B, Maser J, Roehrig C, Paunesku T, Gleber SC, Vine DJ, Finney L, VonOsinski J, Bolbat M, Spink I, Chen Z, Steele J, Trapp D, Irwin J, Feser M, Snyder E, Brister K, Jacobsen C, Woloschak G, Vogt S. 2013. The Bionanoprobe: hard X-ray fluorescence nanoprobe with cryogenic capabilities. J Synchrotron Radiat 21(1):66-75.

Cvetkovic A, Menon AL, Thorgersen MP, Scott JW, Poole II FL, Jenney Jr FE, Lancaster WA, Praissman JL, Shanmukh S, Vaccaro BJ, Trauger SA, Kalisiak E, Apon JV, Siuzdak G, Yannone SM, Tainer JA, Adams MWW. 2010. Microbial metalloproteomes are largely uncharacterized. Nature 466:779-782.

Daims H, Stoecker K, Wagner M. 2005. Fluorescence in situ hybridization for the detection of prokaryotes. In: Osborn AM, Smith CJ, editors. Molecular Microbial Ecology. Abingdon, UK: Bios-Garland. p. 239.

386 Dawson K, Osburn M, Sessions A, Orphan V. 2015. Metabolic associations with archaea drive
387 shifts in hydrogen isotope fractionation in sulfate□reducing bacterial lipids in cocultures
388 and methane seeps. Geobiology 13(5):462-477.
389 Dawson KS, Strąpoć D, Huizinga B, Lidstrom U, Ashby M, Macalady JL. 2012. Quantitative
390 fluorescence in situ hybridization analysis of microbial consortia from a biogenic gas
391 field in Alaska's Cook Inlet Basin. Appl Environ Microbiol 78(10):3599-3605.
392 Demirel B, Scherer P. 2011. Trace element requirements of agricultural biogas digesters during
393 biological conversion of renewable biomass to methane. Biomass Bioenerg. 35:992-998.
394 Diekert G, Konheiser U, Piechulla K, Thauer RK. 1981. Nickel requirement and factor F430
395 content of methanogenic bacteria. J. Bacteriol. 148(2):459-464.
396 Drzyzga O, El Mamouni R, Agathos SN, Gottschal JC. 2002. Dehalogenation of chlorinated
397 ethenes and immobilization of nickel in anaerobic sediment columns under sulfidogenic
398 conditions. Envir Sci Tech 36(12):2630-2635.
399 Ekstrom EB, Morel FMM. 2008. Cobalt limitation of growth and mercury methylation in sulfate-
400 reducing bacteria. Environ Sci Tech 42(1):93-99.
401 Ermler U, Grabarse W, Shima S, Goubeaud M, Thauer RK. 1997. Crystal structure of methyl-
402 coenzyme M reductase: the key enzyme of biological methane formation. Science
403 278(5342):1457-1462.
404 Fahrni CJ. 2007. Biological applications of X-ray fluorescence microscopy: exploring the
405 subcellular topography and speciation of transition metals. Curr Opin Chem Biol
406 11(2):121-127.
407 Fauque GD, Barton LL. 2012. Hemoproteins in dissimilatory sulfate- and sulfur-reducing
408 prokaryotes. Adv Microbiol Physiol 60:1-90.
409 Ferry JG. 2010. How to make a living by exhaling methane. Ann Rev Microbiol 64:453-473.
410 Finke N, Hoehler TM, Jørgensen BB. 2007. Hydrogen 'leakage'during methanogenesis from
411 methanol and methylamine: implications for anaerobic carbon degradation pathways in
412 aquatic sediments. Environ Microbiol 9(4):1060-1071.
413 Florencio L, Field JA, Lettinga G. 1994. Importance of cobalt for individual trophic groups in an
414 anaerobic methanol-degrading consortium. Appl Environ Microbiol 60(1):227-234.
415 Gavel OY, Bursakov SA, Calvete JJ, George GN, Moura JJG, Moura I. 1998. ATP sulfurylases
416 from sulfate-reducing bacteria of the genus *Desulfovibrio*. A novel metalloprotein
417 containing cobalt and zinc. Biochem 37:16225-16232.
418 Gavel OY, Bursakov SA, Rocco GD, Trincao J, Pickering IJ, George GN, Calvete JJ, Shnyrov
419 VL, Brondino CD, Pereira AS. 2008. A new type of metal-binding site in cobalt-and
420 zinc-containing adenylate kinases isolated from sulfate-reducers *Desulfovibrio gigas* and
421 *Desulfovibrio desulfuricans* ATCC 27774. J Inorganic Biochem 102(5):1380-1395.
422 Glass JB, Orphan VJ. 2012. Trace metal requirements for microbial enzymes involved in the
423 production and consumption of methane and nitrous oxide. Front Microbiol 3:61.
424 Glass JB, Yu H, Steele JA, Dawson KS, Sun S, Chourey K, Pan C, Hettich RL, Orphan VJ.
425 2014. Geochemical, metagenomic and metaproteomic insights into trace metal utilization
426 by methane□oxidizing microbial consortia in sulphidic marine sediments. Environ
427 Microbiol 16(6):1592–1611.
428 Gonzalez-Gil G, Kleerebezem R, Lettinga G. 1999. Effects of nickel and cobalt on kinetics of
429 methanol conversion by methanogenic sludge as assessed by on-line CH4 monitoring.
430 Appl Environ Microbiol 65(4):1789–1793.

Gramp JP, Bigham JM, Sasaki K, Tuovinen OH. 2007. Formation of Ni-and Zn-sulfides in cultures of sulfate-reducing bacteria. Geomicrobiol J 24(7-8):609-614.

Gramp JP, Sasaki K, Bigham JM, Karnachuk OV, Tuovinen OH. 2006. Formation of covellite (CuS) under biological sulfate-reducing conditions. Geomicrobiol J 23(8):613-619.

Guss AM, Kulkarni G, Metcalf WW. 2009. Differences in hydrogenase gene expression between *Methanosarcina acetivorans* and *Methanosarcina barkeri*. J Bacteriol 191(8):2826-2833.

Hagemeier CH, Kruer M, Thauer RK, Warkentin E, Ermler U. 2006. Insight into the mechanism of biological methanol activation based on the crystal structure of the methanol-cobalamin methyltransferase complex. Proc Natl Acad Sci 103(50):18917–18922.

Hamann N, Mander GJ, Shokes JE, Scott RA, Bennati M, Hedderich R. 2007. A cysteine-rich CCG domain contains a novel [4Fe-4S] cluster binding motif as deduced from studies with subunit B of heterodisulfide reductase from *Methanothermobacter marburgensis*. Biochemistry 46(44):12875-12885.

Hausrath EM, Liermann LJ, House CH, Ferry JG, Brantley SL. 2007. The effect of methanogen growth on mineral substrates: will Ni markers of methanogen based communities be detectable in the rock record? Geobiology 5(1):49-61.

Ingall ED, Diaz JM, Longo AF, Oakes M, Finney L, Vogt S, Lai B, Yager PL, Twining BS, Brandes JA. 2013. Role of biogenic silica in the removal of iron from the Antarctic seas. Nature Comm 4:1981.

Jansen S, Gonzalez-Gil G, van Leeuwen HP. 2007. The impact of Co and Ni speciation on methanogenesis in sulfidic media—Biouptake versus metal dissolution. Enzyme Microb Tech 40:823-830.

Jansen S, Steffen F, Threels WF, Van Leeuwen HP. 2005. Speciation of Co (II) and Ni (II) in anaerobic bioreactors measured by competitive ligand exchange-adsorptive stripping voltammetry. Environ Sci Tech 39(24):9493-9499.

Karnachuk OV, Sasaki K, Gerasimchuk AL, Sukhanova O, Ivasenko DA, Kaksonen AH, Puhakka JA, Tuovinen OH. 2008. Precipitation of Cu-sulfides by copper-tolerant *Desulfovibrio* isolates. Geomicrobiol J 25(5):219-227.

Kemner KM, Kelly SD, Lai B, Maser J, O'loughlin EJ, Sholto-Douglas D, Cai Z, Schneegurt MA, Kulpa CF, Nealson KH. 2004. Elemental and redox analysis of single bacterial cells by X-ray microbeam analysis. Science 306(5696):686-687.

Krumholz LR, Elias DA, Suflita JM. 2003. Immobilization of cobalt by sulfate-reducing bacteria in subsurface sediments. Geomicrobiol J 20(1):61-72.

Loy A, Lehner A, Lee N, Adamczyk J, Meier H, Ernst J, Schleifer K-H, Wagner M. 2002. Oligonucleotide microarray for 16S rRNA gene-based detection of all recognized lineages of sulfate-reducing prokaryotes in the environment. Appl Environ Microbiol 68(10):5064-5081.

Luther III GW, Rickard DT. 2005. Metal sulfide cluster complexes and their biogeochemical importance in the environment. J Nanopart Res 7(4-5):389-407.

Macalady JL, Lyon EH, Koffman B, Albertson LK, Meyer K, Galdenzi S, Mariani S. 2006. Dominant microbial populations in limestone-corroding stream biofilms, Frasassi cave system, Italy. Appl Environ Microbiol 72(8):5596-5609.

Mayr S, Latkoczy C, Kruger M, Gunther D, Shima S, Thauer RK, Widdel F, Jaun B. 2008. Structure of an F430 variant from archaea associated with anaerobic oxidation of methane. J Am Chem Soc 130(32):10758-10767.

McGlynn SE, Chadwick GL, Kempes CP, Orphan VJ. 2015. Single cell activity reveals direct electron transfer in methanotrophic consortia. Nature 526:531–535.

Moreau JW, Fournelle JH, Banfield JF. 2013. Quantifying heavy metals sequestration by sulfate-reducing bacteria in an acid mine drainage-contaminated natural wetland. Front Microbiol 4:43.

Moreau JW, Webb RI, Banfield JF. 2004. Ultrastructure, aggregation-state, and crystal growth of biogenic nanocrystalline sphalerite and wurtzite. Am Mineral 89(7):950-960.

Moreau JW, Weber PK, Martin MC, Gilbert B, Hutcheon ID, Banfield JF. 2007. Extracellular proteins limit the dispersal of biogenic nanoparticles. Science 316(5831):1600-1603.

Nuester J, Vogt S, Newville M, Kustka AB, Twining BS. 2012. The unique biochemical signature of the marine diazotroph *Trichodesmium*. Front Microbiol 3:1-15.

Oremland RS, Polcin S. 1982. Methanogenesis and sulfate reduction: competitive and noncompetitive substrates in estuarine sediments. Appl Environ Microbiol 44(6):1270-1276.

Osburn MR, Dawson KS, Fogel ML, Sessions AL. 2016. Fractionation of hydrogen isotopes by sulfate-and nitrate-reducing bacteria. Front Microbiol 7.

Outten CE, O'Halloran TV. 2001. Femtomolar sensitivity of metalloregulatory proteins controlling zinc homeostasis. Science 292(5526):2488-2492.

Ozuolmez D, Na H, Lever MA, Kjeldsen KU, Jørgensen BB, Plugge CM. 2015. Methanogenic archaea and sulfate reducing bacteria co-cultured on acetate: teamwork or coexistence? Front Microbiol 6:492.

Paulo LM, Stams AJ, Sousa DZ. 2015. Methanogens, sulphate and heavy metals: a complex system. Rev Environ Sci Biotech 14(4):537-553.

Paulo PL, Jiang B, Cysneiros D, Stams AJM, Lettinga G. 2004. Effect of cobalt on the anaerobic thermophilic conversion of methanol. Biotech Bioeng 85(4):434-441.

Pereira IAC, Ramos AR, Grein F, Marques MC, Da Silva SM, Venceslau SS. 2011. A comparative genomic analysis of energy metabolism in sulfate reducing bacteria and archaea. Front Microbiol 2(69):1-22.

Phelps T, Conrad R, Zeikus J. 1985. Sulfate-dependent interspecies H2 transfer between *Methanosarcina barkeri* and *Desulfovibrio vulgaris* during coculture metabolism of acetate or methanol. Appl Environ Microbiol 50(3):589-594.

Price NM, Harrison GI, Hering JG, Hudson RJ, Nirel PM, Palenik B, Morel FM. 1988. Preparation and chemistry of the artificial algal culture medium Aquil. Biol Oceanogr 6(5-6):443-461.

Ragsdale SW, Kumar M. 1996. Nickel-containing carbon monoxide dehydrogenase/acetyl-CoA synthase. Chem Rev 96(7):2515-2540.

Raskin L, Poulsen LK, Noguera DR, Rittmann BE, Stahl DA. 1994. Quantification of methanogenic groups in anaerobic biological reactors by oligonucleotide probe hybridization. Appl Environ Microbiol 60(4):1241-1248.

Rouf M. 1964. Spectrochemical analysis of inorganic elements in bacteria. J Bacteriol 88(6):1545-1549.

Scherer P, Lippert H, Wolff G. 1983. Composition of the major elements and trace elements of 10 methanogenic bacteria determined by inductively coupled plasma emission spectrometry. Biol Trace Elem Res 5(3):149-163.

Scherer P, Sahm H. 1981. Effect of trace elements and vitamins on the growth of *Methanosarcina barkeri*. Acta Biotechnol 1(1):57-65.

Schmidt H, Eickhorst T, Mußmann M. 2012. Gold-FISH: a new approach for the in situ detection of single microbial cells combining fluorescence and scanning electron microscopy. System Appl Microbiol 35(8):518-525.

Sitte J, Pollok K, Langenhorst F, Küsel K. 2013. Nanocrystalline nickel and cobalt sulfides formed by a heavy metal-tolerant, sulfate-reducing enrichment culture. Geomicrobiol J 30(1):36-47.

Spanjers H, Weijma J, Abusam A. 2002. Modelling the competition between sulphate reducers and methanogens in a thermophilic methanol-fed bioreactor. Water Sci Tech 45(10):93-98.

Stams AJ, Plugge CM. 2009. Electron transfer in syntrophic communities of anaerobic bacteria and archaea. Nat Rev Microbiol 7(8):568-577.

Thauer RK, Kaster A-K, Goenrich M, Schick M, Hiromoto T, Shima S. 2010. Hydrogenases from methanogenic archaea, nickel, a novel cofactor, and H2 storage. Ann Rev Biochem 79:507-536.

Thauer RK, Kaster A-K, Seedorf H, Buckel W, Hedderich R. 2008. Methanogenic archaea: ecologically relevant differences in energy conservation. Nat Rev Microbiol 6:579-591.

Twining BS, Baines SB, Fisher NS, Maser J, Vogt S, Jacobsen C, Tovar-Sanchez A, Sanudo-Wilhelmy SA. 2003. Quantifying trace elements in individual aquatic protist cells with a synchrotron X-ray fluorescence microprobe. Anal Chem 75(15):3806-3816.

Twining BS, Baines SB, Vogt S, de Jonge MD. 2008. Exploring ocean biogeochemistry by single-cell microprobe analysis of protist elemental composition. J Eukaryot Microbiol 55(3):151-162.

van Hullebusch ED, Gieteling J, Zhang M, Zandvoort MH, Daele WV, Defrancq J, Lens PNL. 2006. Cobalt sorption onto anaerobic granular sludge: Isotherm and spatial localization analysis. J Biotechnol 121(2):227-240.

van Hullebusch ED, Peerbolte A, Zandvoort MH, Lens PNL. 2005. Sorption of cobalt and nickel on anaerobic granular sludges: isotherms and sequential extraction. Chemosphere 58(4):493-505.

van Hullebusch ED, Zandvoort MH, Lens PNL. 2004. Nickel and cobalt sorption on anaerobic granular sludges: kinetic and equilibrium studies. J Chem Tech Biotech 79(11):1219-1227.

Vogt S. 2003. MAPS: A set of software tools for analysis and visualization of 3D X-ray fluorescence data sets. J Phys IV 104:635-638.

Weijma J, Stams A. 2001. Methanol conversion in high-rate anaerobic reactors. Water Sci Tech 44(8):7-14.

Xu J, Murayama M, Roco CM, Veeramani H, Michel FM, Rimstidt JD, Winkler C, Hochella MF. 2016. Highly-defective nanocrystals of ZnS formed via dissimilatory bacterial sulfate reduction: A comparative study with their abiogenic analogues. Geochem Cosmochim Acta 180:1-14.

Zandvoort MH, Geerts R, Lettinga G, Lens PNL. 2003. Methanol degradation in granular sludge reactors at sub-optimal metal concentrations: role of iron, nickel and cobalt. Enzyme Microbiol Tech 33(2-3):190-198.

Zandvoort MH, van Hullebusch ED, Gieteling J, Lens PNL. 2006. Granular sludge in full-scale anaerobic bioreactors: trace element content and deficiencies. Enzyme Microbiol Tech 39(2):337-346.

567 Zhang Y, Gladyshev VN. 2010. dbTEU: a protein database of trace element utilization.
568 Bioinformatics 26(5):700-702.
569 Zhang Y, Rodionov DA, Gelfand MS, Gladyshev VN. 2009. Comparative genomic analyses of
570 nickel, cobalt and vitamin B12 utilization. BMC Genomics 10(78):1-26.

571

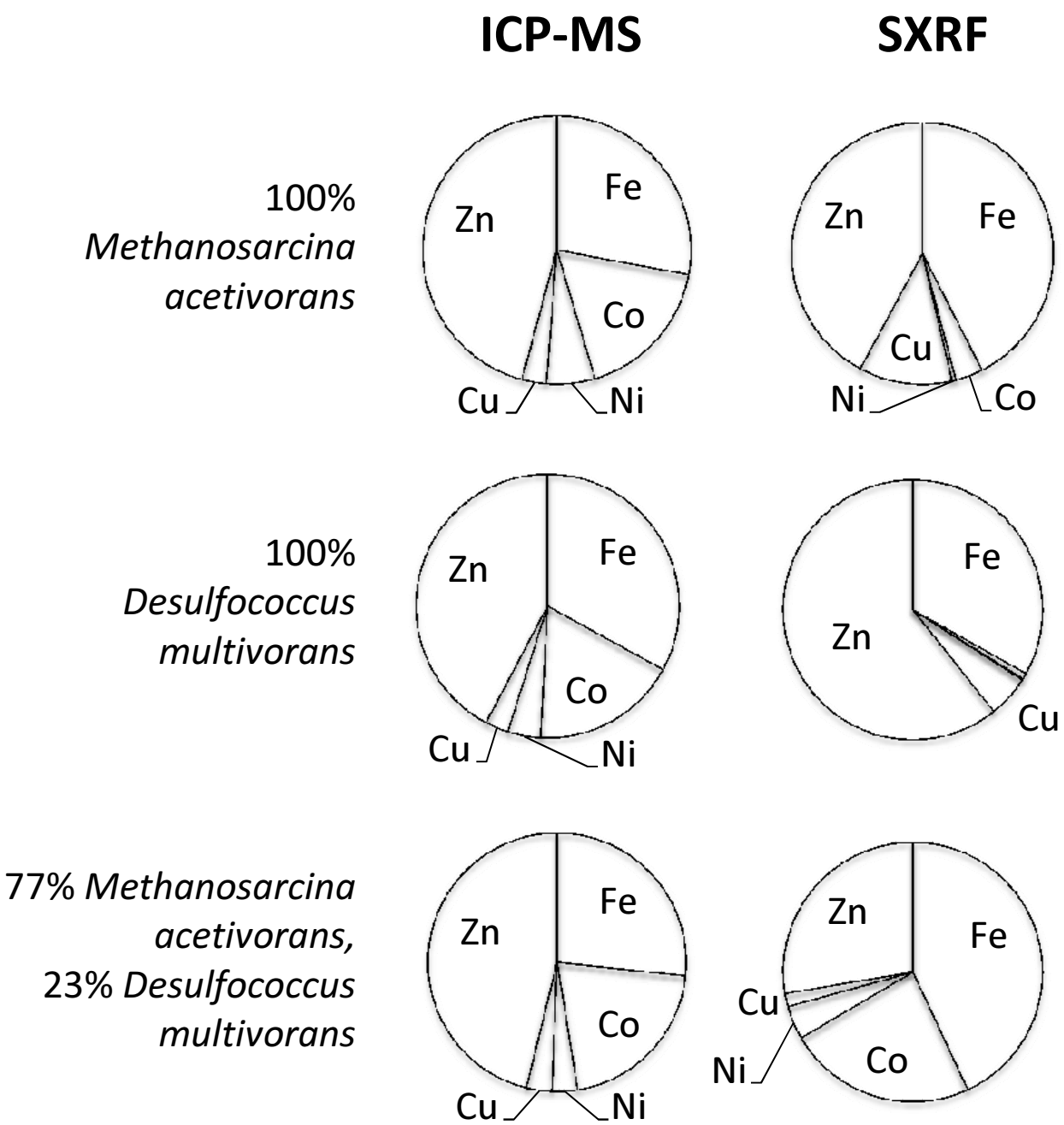

10 μm

Figure 2

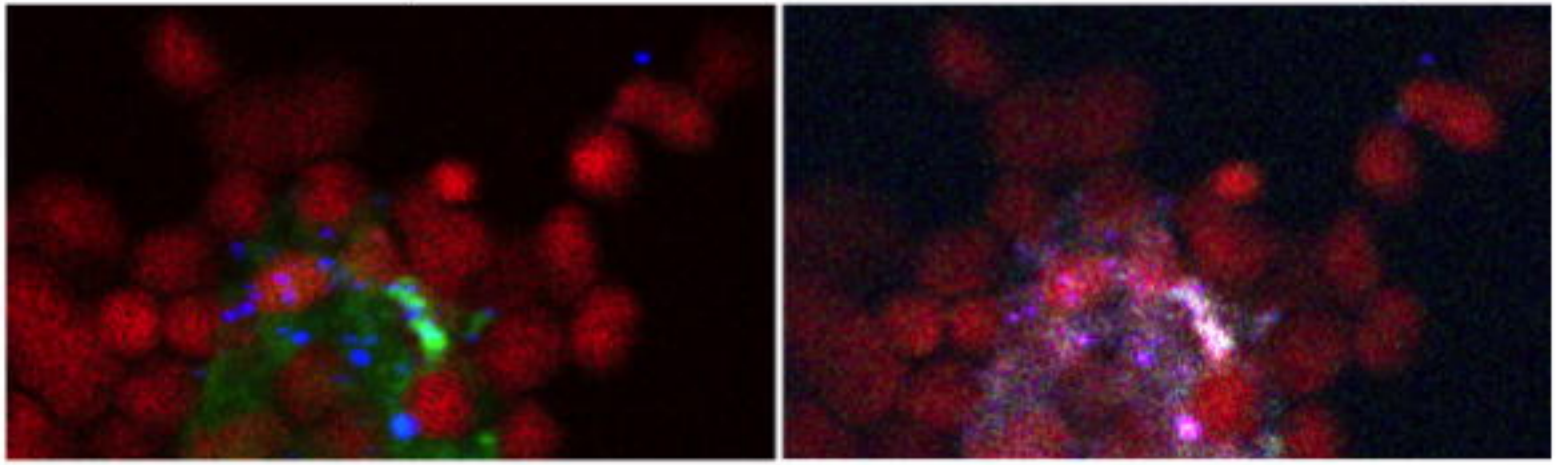

P (3.5) Co (0.4) Zn (0.7)

S (2.7) Ni (0.03) Cu (0.04)

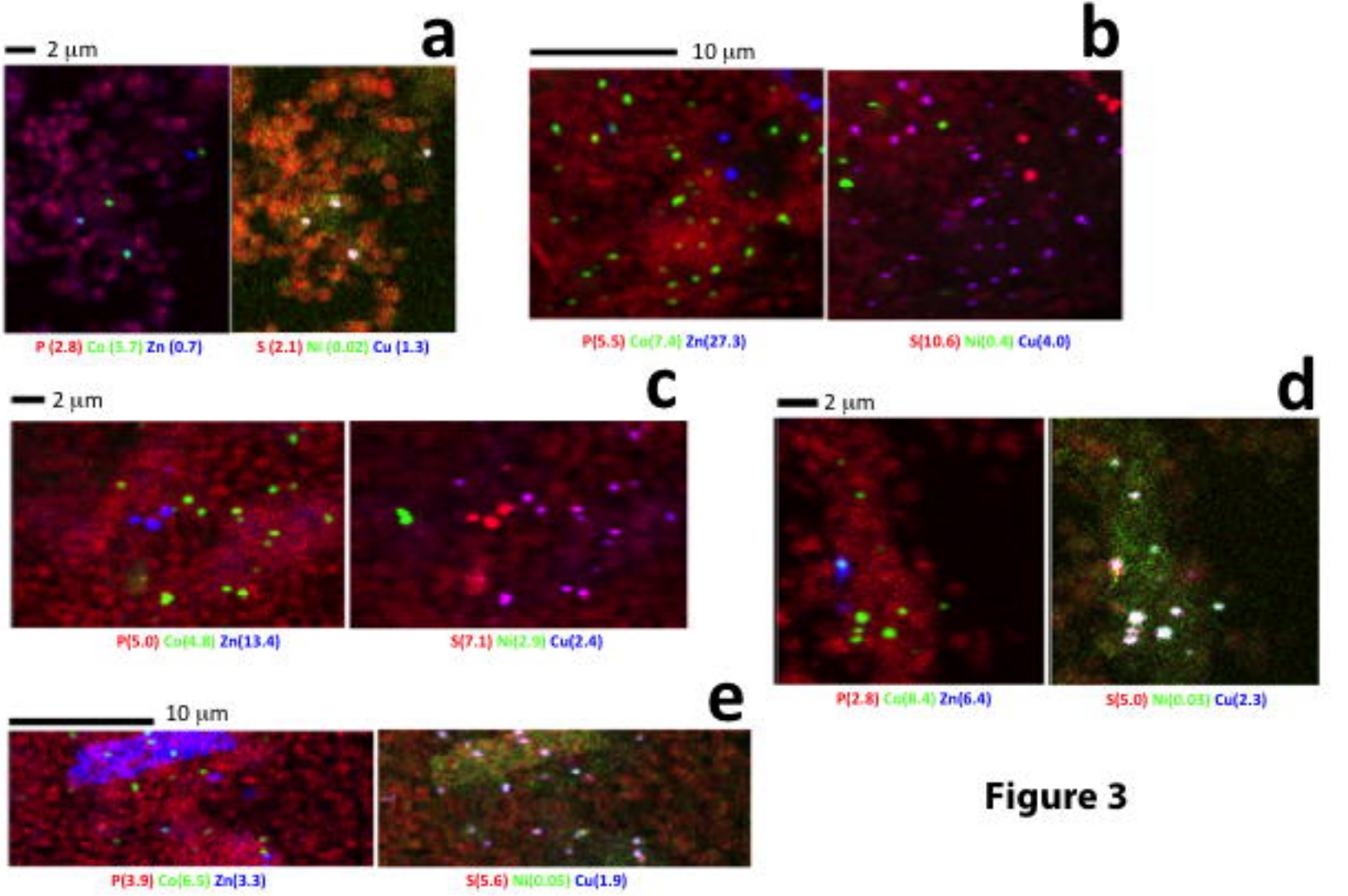
a
2 μm
P (2.8) Co (5.7) Zn (0.7)
S (2.1) Ni (0.02) Cu (1.3)
b
10 μm
P(5.5) Co(7.4) Zn(27.3)
S(10.6) Ni(0.4) Cu(4.0)
c
2 μm
P(5.0) Co(4.8) Zn(13.4)
S(7.1) Ni(2.9) Cu(2.4)
d
2 μm
P(2.8) Co(8.4) Zn(6.4)
S(5.0) Ni(0.03) Cu(2.3)
e
10 μm
P(3.9) Co(6.5) Zn(3.3)
S(5.6) Ni(0.05) Cu(1.9)

Figure 3

Desulfococcus multivorans

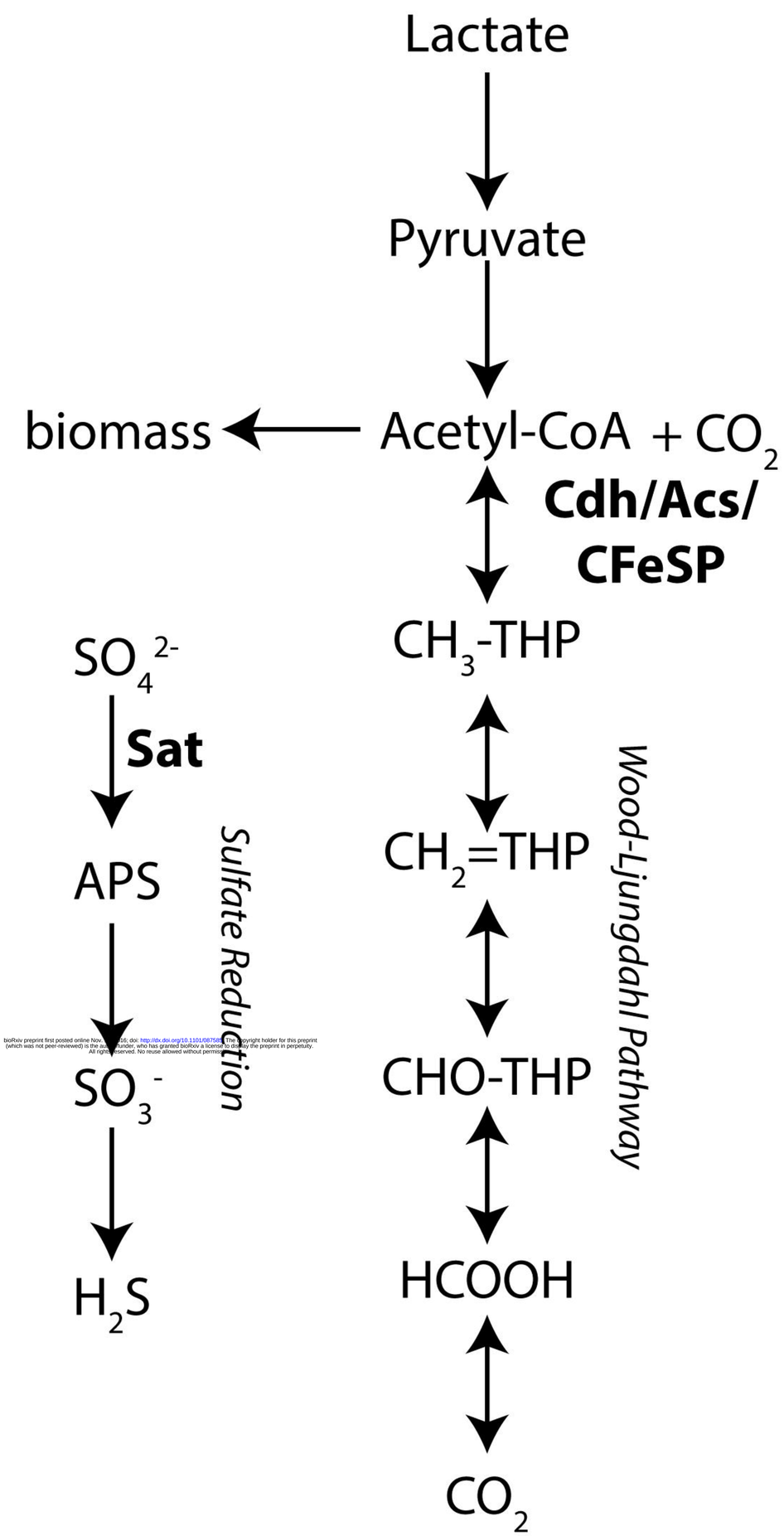

Methanosarcina acetivorans C2A